RESEARCH COMMUNICATION

Loss of Runt-Related Transcription Factor 3 Expression Associated with Human Hepatocellular Carcinoma Progression and Prognosis

Jianguo Li[1]*, Xiaojie Jiang[2]

Abstract

Background: This study aimed to evaluate the expression level of runt-related transcription factor 3 (RUNX3) in human primary hepatocellular carcinomas (HCCs) and its relationship with the clinic pathological features. Methods: RUNX3 expression was analyzed by real-time fluorescent quantitative PCR, immunohistochemistry and Western blotting in HCC cells and tissues. Results: RUNX3 mRNA and protein expression was decreased in HCC tissues compared with the adjacent normal tissues (P< 0.001), mRNA frequently being down-regulated in HCC cell lines (66.7%, 4/6). Low expression of RUNX3 showed a significant correlation with cirrhosis (P = 0.028), histologic type (P = 0.000) and lymph node metastasis (P = 0.004). Conclusion: RUNX3 expression is deleted or decreased in HCCs and cell lines, in association with progression and prognosis.

Key words: Runt-related transcription factor 3 - HCC - fluorescent quantitative PCR - gene expression

Asian Pacific J Cancer Prev, **12**, 2285-2290

Introduction

Hepatocellular carcinoma (HCC) is the sixth most common cancer and prevalent cancers in the human population, more than 50% of the world´s HCC cases occur in China (EI-Serag and Rudolph, 2007; Zhang et al., 2009). It is well known that numerous genetic abnormalities have been associated with cancer development. However, the knowledge about the molecular genetics event in the progression and prognosis of HCC has been limited. Therefore, it is important to detect the molecular mechanism involved in the development of HCC.

The human runt-related transcription factor 3 (RUNX3), located at 1p36.1, encodes a protein that has several functions in human development and in regulating organization (Bangsow et al., 2001). Recent studies have revealed that RUNX3 plays an important role in TGF-βsignaling pathway. In this pathway, Smad2 and Smad3 activated by TGF-βinteract with RUNX3, and induce transcriptional activation of target genes in the nucleus (Ito and Miyazono, 2003; Miyazono et al., 2003; Chi et al., 2005). RUNX3 overexpression was frequently observed and was well correlated with malignant behaviors in head and neck cancer, promoted cell growth and inhibited apoptosis in head and neck cancer cells (Kudo et al., 2011). Moreover, some reports suggest that RUNX3 is frequently inactivated in various carcinomas, including gastric (Sakakura et al., 2005), breast (Hussenet et al., 2007), colon (Goel et al., 2004), head and neck cancer (Tsunematsu et al., 2009).The loss or decrease of RUNX3 expression in HCC tissue has been recently reported (Nakanishi et al., 2011; Shiraha et al., 2011; Li et al., 2008). However, due to the limited specimens, it is necessary to enlarge the samples to demonstrate the relationship between RUNX3 expression and HCC, analyze the relationship between RUNX3 expression and clinicopathological features in HCC.

Materials and Methods

Cell lines and culture

The HCC cell lines BEL7402, SMMC-7721, PLC, QGY-7701, HepG2 and Hep3B) and human normal liver cell line (HL-7702) were obtained from Chinese Academy of Sciences, Shanghai, China. All cell lines were cultured in RPMI Medium 1640 (Invitrogen, Carlsbad, CA, USA) supplemented with 10% fetal bovine serum. Cells were incubated at 37°C in a humidified atmosphere of 5% CO_2 in air.

Patients and surgical specimens

Sixty-five patients with primary HCC who

*[1]Department of Hepatobiliary Surgery, Zhangzhou Affiliated Hospital, Fujian Medical University, Zhangzhou, [2]Department of Oncological Surgery, Putian Affiliated Hospital, Putian University, China *For correspondence: jianguoli163@163.com*

underwent surgery at Zhangzhou Affiliated Hospital of Fujian Medical University between January 2008 and December 2009 were included in this study. Samples collected were stored immediately in liquid nitrogen at -80°C until analysis. The median age of the patients was 55.9 ± 8.5 years (range, 30-72 years). The ratio of male to female was 48:17. Information on gender, age, stage of disease, and histopathologic factors was obtained from the medical records. All of the tumors were confirmed as HCC by the Clinicopathologic Department. All patients gave informed consent approved by our ethics committee for use of all specimens.

PCR analysis

Total RNA was isolated from the tumor specimens, adjacent normal liver tissues of 65 patients, and seven cells lines with Trizol reagent (Invitrogen, USA). Preparations were quantified and their purity was determined by standard spectrophometric methods. Reverse transcription was performed using random primers and RevertAid™ First Strand cDNA Synthesis Kit (Fermentas) and stored at -20 °C until using.

Quantitative real-time PCR was performed on GeneAmp®PCR System 9700 PCR instrument (Applied Biosystems Corporation) in triplicate in a 15-μl volume in 96-well plates. PCR amplification of RUNX3 was performed using forward prime: 5´-GGTGAAGTCTTGCCCCTG AA-3´and reverse primer: 5´-ATGAGTTCCCTTACGCCTTTT-3´(product 128bp).β-actin was used as an internal control. Primer sequences for β-actin were 5´-ACG TGG ACA TCC GCA AAG AC -3´(forward) and 5´-CAA GAA AGG GTG TAA CGC AAC TA-3´(reverse) (308 bp). Each reaction included 7.5 μl of 2×Maxima™ SYBR-Green qPCR Master Mix (Fermentas), 0.5 μl of forward primer, 0.5 μl of reverse primer, 6 μl of template cDNA and 0.5 μl of nuclease-free water. The PCR amplification cycles consisted of an initial denaturation at 95°C for 10 min, 42 cycles of denaturation at 95°C for 10 sec, annealing at 57°C for 20 sec, and extension at 72°C for 1 min. The comparative cycle threshold (Ct) method (2--Ct) was established for the relative quantification of RUNX3 expression [11]. The dissociation of SYBR Green-labeled cDNA was carried out after completion of real-time PCR by heating the products for 5 sec at 95°C, 5 sec at 55°C and then slowly increasing temperature up to 95°C at least 20 min. The dissociation curve for each amplification cycle was analyzed to confirm that there were no non-specific PCR products. The amplification reaction products were resolved on 1.5% agarose gels and visualized by ethidium-bromide staining.

Immunohistochemical staining

Formalin-fixed and paraffin-embedded sections (4 mm thick) were cut and mounted on aminopropyltriethoxysilane-treated slides. The slides were routinely deparaffinized with xylene and rehydrated with a series of ethanol washing. Endogenous peroxidase activity was blocked by incubation in 3% hydrogen peroxide methanol for 10 min. After washing with phosphate-buffered saline (PBS), the sections were subjected to antigen retrieval in boiling sodium citrate buffer (0.01 mM; pH 6.0) for 10 min in a microwave oven set at 95–100°C After the sections were cooled at room temperature, the specimens were saturated in 10% normal goat serum (S-P immunohistochemical kit; Fujian Maixin Biological Technology Ltd., Fujian, China) for 5 min and incubated at room temperature for 60 min with the primary antibody, the goat antihuman RUNX3 (dilution 1:400, Santa Cruz Biotech, USA). After the sections were washed with PBS, a biotinylated rabbit antibody to goat immunoglobulin (S-P immunohistochemical kit) was applied, followed by incubation at room temperature for 10 min. Immunohistochemical reactions were developed in freshly prepared 3,30-diamino-benzidine tetrahydrochloride (DAB kit; Fujian Maixin Biological Technology Ltd.) for immune complex visualization and then counterstained with hematoxylin for 30 sec. Slides were counterstained in hematoxylin and dehydrated through a graded alcohol series terminating with xylene. Formalin-fixed and paraffin-embedded sections of human liver tissues with strong staining served as a positive control and PBS in lieu of antihuman RUNX3 as a negative control. Stained slides were examined microscopically by two immunohistochemistry experts. The sections were scored on a four-tier scale; 0, negative; 1, weak signal; 2, intermediate signal; and 3, strong signal.

Western blot analysis

HCC tissues and adjacent non-tumor tissues were lysed in the sample buffer [2% SDS, 10% glycerol, and 50 mM of Tris-HCl (pH 6.8)] at room temperature. The lysates were sonicated and the protein concentration was estimated by the Bradford method using BCA Protein Assay Reagent (Pierce, Rockford, MA, USA). 50 μg of lysates were electrophoresed on 12 % SDS-PAGE and transferred to polyvinylidene difluoride membranes (Immobilon; Millipore, Bedford, MA, USA).The membranes were then blocked with TBS [20 mM Tris, 150 mM NaCl (pH 7.6)] containing 5 % skim milk and 0.1% Tween 20 for 1 h and incubated for 12 h at 4°C with the goat anti-human RUNX3 affinity purified polyclonal antibody (dilution 1:500, Santa Cruz Biotech, USA). The membranes were subsequently incubated at room temperature for 2 h with horseradish peroxidase (HRP) conjugated donkey anti-goat secondary antibodies (dilution 1:1000) and analyzed using an enhanced chemiluminescence system (Beyotime, Jiangsu, China).

Statistical analysis

The data were expressed as means±(standard deviation) SD. Data consisting of continuous variables

were analyzed by the independent-sample t-test for two groups, and least-significant difference (LSD) for three groups. Statistical analyses were performed with SPSS ver.13.0 software. A probability value (P-value) less than 0.05 was considered statistically significant.

Results

RUNX3 mRNA expression in HCC and adjacent non-tumor tissues

The optical density (OD) value at 260 and 280 nm of extracted RNA determined by ultraviolet spectrophotometer showed that OD26/OD280 was less than 1.75. The formaldehyde-denatured agarose gel electrophoresis of RNA showed three bands and the ratio of 28s and 18s was about 2:1, which indicated that the total RNA was integrated without obvious degradation.

RT-PCR results of HCC and the normal tissues shown that two clear and specific bands were detected in the 1.5% agarose gel (Figure 1), which matched the length of target gene RUNX3 (129 bp) and the control gene β-actin (308 bp).

The amplification curves describing the dynamic process of real-time PCR for β-actin indicated good fluorescence signals (Figure 2A). In addition, the melting curve of quantitative PCR product of RUNX3 showed that one clearly prominent peak was observed

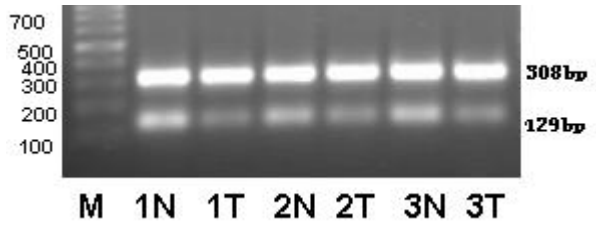

Figure 1. Detection of RUNX3 Transcripts (129 bp) in HCC and Adjacent Normal Tissues by RT-PCR. β-actin was used as a control (308 bp). M: DNA marker. 1N, 2N, 3N normal and 1T, 2T, 3T tumor tissues

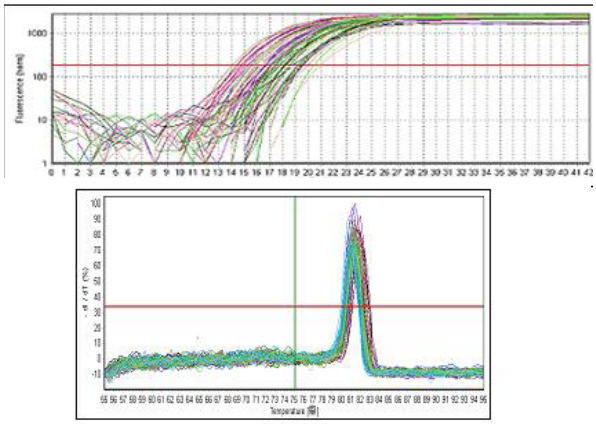

Figure 2. Real-time PCR Amplification Curves o β-actin and RUNX3. a) Real-time PCR amplificatio curves of β-actin; b) Melting curves of RUNX3 by quantitative PCR. One significantly peak was observed in the curve, indicating the amplified product was specific

Table 1. Comparison of RUNX3 mRNA Expression Between HCC and Adjacent Nomal Tissue

	N. of cases	RUNX3 mRNA(CT)	2^{CT}	P
HCC	65	9.42±1.80		
Non-tumor	65	7.34±1.80	0.24	0.000

in the curve, indicating primer dimmer or nonspecific amplified product was rarely produced (Figure 2B).

The relative quantification of RUNX3 mRNA expression in HCC and adjacent non-tumor tissues were further analyzed (Table 1). The results indicated that RUNX3 expression was decreased compared to adjacent normal tissues ($P < 0.05$). The RUNX3 mRNA levels were 9.42±1.80, 7.34±1.80 in HCC and adjacent normal tissues, respectively. The mRNA RUNX3 expression in HCC was 4.2-fold lower than that in adjacent normal tissues, the difference was significant between them ($P < 0.001$), which indicated RUNX3 mRNA was down-regulated in HCC compared to that in adjacent non-tumor tissues.

RUNX3 mRNA expression in human liver cell lines

As shown in Figure 3, RUNX3 mRNA expression in four human liver tumor cell lines (66.67%, 4/6 QGY-7701, HEPG2, Hep3B, and BEL-7402) showed 3-8 fold significantly lower expression than that in the human normal liver cell line (HL-7702). There was no significant down-regulation of RUNX3 in the other two liver tumor cell lines (SMMC-7721 and PLC).

RUNX3 protein expression in HCC and adjacent non-tumor tissues

RUNX3 protein expression in 65 HCC tissues and adjacent non-tumor tissues was determined by Western blot (Figure 4). In accordance with the mRNA analysis,

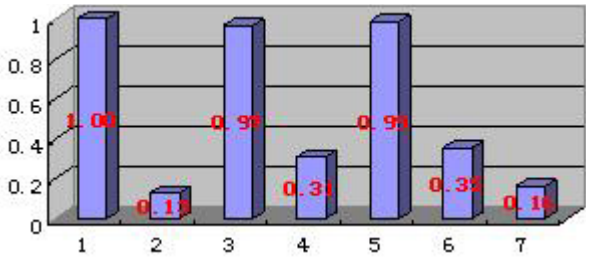

Figure 3. Comparison of RUNX3 mRNA Expression in Cell Lines. 1 normal cell line HL-7702. 2-7: HCC lines QGY-7701, SMMC-7721, HEPG2, PLC, Hep3B, BEL-7402

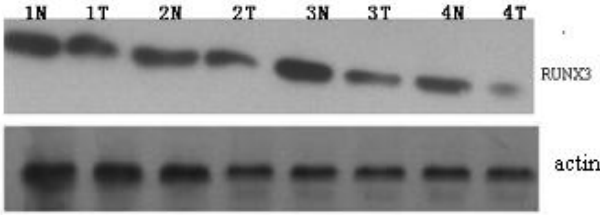

Figure 4. Expression of RUNX3 Protein in HCC and Adjacent Non-tumor Tissues

Table 2. Relationship Between RUNX3 mRNA Expression and Clinicopathologic Characteristics in 65 Patients

Variables	N. of cases (%)	RUNX3 mRNA (2^{-Ct})	P
Sex			
Male	48	0.7113±1.2890	
Female	17	0.3401±0.3161	0.247 [a]
Age at diagnosis			
<50years	21	0.4659±0.8079	
≥50years	44	0.6850±1.2549	0.468 [a]
Tumor site			
<5cm	29	0.6591±1.0470	
≥5cm	36	0.5780±1.2029	0.776 [a]
Serum HbsAg			
Negative	24	0.7856±1.1135	
Positive	41	0.5139±1.1380	0.353 [a]
Liver cirrhosis			
Negative	22	1.1722±1.6296	
Positive	43	0.3288±0.6040	0.028 [a]*
Histologic type			
Well diff	11	2.0868±2.1288	
Mod diff	34	0.4194±0.4215	
Poor diff	20	0.1355±0.1686	0.000 [b]*
TNM stage			
I~II	38	0.6825±1.2844	
III~IV	27	0.5181±0.8767	0.567 [a]
Portal vein invasion			
Negative	39	0.6558±1.2621	
Positive	26	0.5518±0.9111	0.719 [a]
Lymph node metastasis			
Negative	47	0.7769±1.2888	
Positive	18	0.1895±0.0425	0.004 [a]*

[a]Statistical significance was evaluate by independent-sample t-test; [b]Statistical significance was evaluate by LSD (well differentiated HCC vs. moderately differentiated, P = 0.000, well differentiated HCC vs. poorly differentiated, P = 0.000, moderately differentiated HCC vs. poorly differentiated, P = 0. 274); * P < 0.05

RUNX3 expression is decreased in HCC tissues compared with the adjacent normal tissues. There was significant difference in the level of RUNX3 expression between the HCC and the adjacent non-tumor tissues (P<0.05).

To further assess the RUNX3 expression in HCC, immunohistochemistry was performed. RUNX3 expression was mainly present in the cell cytoplasm. Strong signal was detected in the adjacent non-tumor tissues under microscopy, only weak signal could be detected in HCC (Figure 5).

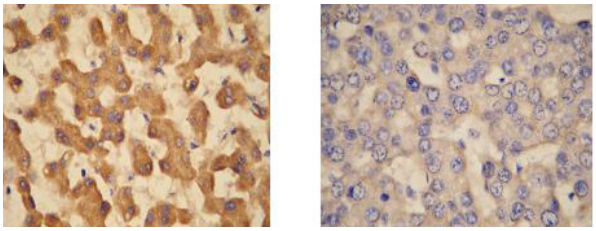

Figure 5. Immunohistochemical Staining of RUNX3. a) Non-tumor liver tissue with a protein score of 3; b)HCC tissue with a protein score of 0

Correlation between RUNX3 mRNA expression and clinicopathologic factors

We found that statistically significant relationship exists between low RUNX3 mRNA levels and liver cirrhosis (P < 0.05). The expression level of RUNX3 was lower in the cirrhosis group than that in the negative group (Positive cirrhosis HCC vs. negative cirrhosis, P = 0.028). LSD also showed significant differences in mRNA expression among the HCC (well differentiated HCC vs. moderately differentiated, P = 0.000; well differentiated HCC vs. poorly differentiated, P = 0.000; moderately differentiated HCC vs. poorly differentiated P = 0.274). Furthermore, significantly statistical relationship was also found between lower RUNX3 mRNA levels and lymph node metastasis (P = 0.004). Except that, no correlation was observed between RUNX3 mRNA levels and the studied clinicopathologic factors (Table 2).

Discussion

In the present study, we confirmed the RUNX3 expression decreased in HCC tissues and liver tumor lines. The mRNA expression level of RUNX3 in HCC tissues showed 4.2-fold significantly lower than that in adjacent non-tumor tissues by relative quantitative RT-PCR analysis. RUNX3 showed 3 to 8-fold significantly lower expression in live tumor cell lines QGY-7701, HEPG2, Hep3B and BEL-7402 compared with live normal cell lines HL-7702. Both of them indicated that RUNX3 mRNA expression levels were significantly lower in HCC (P < 0.001), which was concordant with some previous studies in various tumor (Shiraha et al., 2011; Li et al., 2008; Livak and Schmittgen, 2001; Mori et al., 2005; Wei et al., 2005; He et al., 2008). Furthermore, Western blot analysis showed that there was also significant difference in RUNX3 protein expression between the HCC and adjacent non-tumor tissues, which was accordant with our results of RUNX3 mRNA analysis. Taken together, we consider that the low expression of RUNX3 may play some vital roles in the development of the HCC.

The role of cirrhosis as a precancerous lesion of HCC has been widely accepted. According to our statistical analysis of clinicopathological data, the expression level of RUNX3 was lower in cirrhosis group than that in negative group. These results contribute to the evidence of RUNX3 participating in the development of cirrhosis, and the down-expression of RUNX3 may be an early event in HCC.

The methylation status of RUNX3 in colorectal cancers is correlated with the cancer differentiation (Li et al., 2002; Jiang et al., 2008). The lower RUNX3 levels were associated with poorly differentiated types (P = 0.049) (Lee, 2011; Imamura et al., 2005; Araki et al., 2005). Their findings were concordant with our results in HCC. Our present data demonstrated that

RUNX3 mRNA expression levels in well, moderately and poorly differentiated HCC tissues were 2.0868 ± 2.1288, 0.4194 ± 0.4215 and 0.1355 ± 0.1686, respectively. LSD showed significant differences in mRNA expression among the HCC (well differentiated HCC vs. moderately differentiated, P = 0.000; well differentiated HCC vs. poorly differentiated, P = 0.000; moderately differentiated HCC vs. poorly differentiated P = 0.274). This result suggests that the levels of RUNX3 mRNA expression were markedly correlated with the HCC differentiation (P <0.05), and the level of RUNX3 mRNA was lower in poorly differentiated tumors than that in well and moderately differentiated tumors. Thus, decreased expression of RUNX3 could be a further factor to detect the histotype of HCC. In addition, statistically significant links were found between lower RUNX3 mRNA levels and lymph node metastasis (0.7769 ± 1.2888 vs. 0.1895 ± 0.0425, P = 0.004), the expression of RUNX3 mRNA was lower in the presence of lymph node metastasis than that in their absence. It revealed that the RUNX3 mRNA levels may be as an important indicator of prognosis in HCC patients. Except these, no correlation was observed between RUNX3 mRNA levels and the studied clinicopathological factors.

In conclusion, lower expression of RUNX3 might be a potential mechanism of HCC development and there is a significant correlation between RUNX3 and some clinical features of patients such as cirrhosis, histologic type and lymph node metastasis. However, the details of biological RUNX3 functions in HCC are unclear and coherent molecular explanation has not yet to be reported. Therefore further biochemical and biological studies are required to elucidate the detailed mechanisms and to clarify the value of adopting biological prognostic factors into clinical practice.

Acknowledgments

We are particularly grateful to Dr. Xiao-lang Wang and Dr. Chong-zhi Zhou from Shanghai First People's Hospital of Jiao Tong University for ideas and help. This work was supported by National Natural Science Foundation of Fujian Province, China. The authors state no competing interests.

References

Araki K, Osaki M, Nagahama Y, et al (2005). Expression of RUNX3 protein in human lung adenocarcinoma: implications for tumor progression and prognosis. *Cancer Sci*, **96**, 227-31.

Bangsow C, Rubins N, Glusman G, et al (2001). The RUNX3 gene--sequence, structure and regulated expression. *Gene*, **279**, 221-32.

Chi XZ, Yang JO, Lee KY, et al (2005). RUNX3 suppresses gastric epithelial cell growth by inducing p21 (WAF/Cip1) expression in cooperation with transforming growth factor {beta}-activated SMAD. *Mol Cell Biol*, **25**, 8097-107.

EI Serag HB, Rudolph KL (2007). Hepatocellular carcinoma: epidemiology and molecular carcinogenesis. *Gastroenterol*, **132**, 2557-76.

Goel A, Arnold CN, Tassone P, et al (2004). Epigenetic inactivation of RUNX3 in microsatellite unstable sporadic colon cancers. *Int J Cancer*, **112**, 254-9.

He JF, Ge MH, Zhu X, et al (2008). Expression of RUNX3 in salivary adenoid cystic carcinoma: Implications for tumor progression and prognosis. *Cancer Sci*, **99**, 1334-40.

Hussenet T, Han W, Bae JY, et al (2007). Downregulation of the RUNX3 gene by promoter hypermethylation and hemizygous deletion in breast cancer. *J Korean Med Sci*, **22**, 24-31.

Imamura Y, Hibi K, Koike M, et al (2005). RUNX3 promoter region is specifically methylated in poorly-differentiated colorectal cancer. *Anticancer Res*, **25**, 2627-30.

Ito Y, Miyazono K (2003). RUNX transcription factors as key targets of TGF-β superfamily signaling. *Curr Opin Genet Dev*, **13**, 43-7.

Jiang Y, Tong DD, Lou G, et al (2008). Expression of RUNX3 gene, methylation status and clinicopathological significance in breast cancer and breast cancer cell lines. *Pathobiology*, **75**, 244-51.

Kudo Y Tsunematsu T, Takata T (2011). Oncogenic role of RUNX3 in head and neck cancer. *J Cell Biochem*, **112**, 383-93.

Lee YM (2011). Control of RUNX3 by histone methyltransferases. *J Cell Biochem*, **112**, 394-400.

Li QL, Ito K, Sakakura C, et al (2002). Causal relationship between of the loss of RUNX3 expression and gastric cancer. *Cell*, **109**, 113-24.

Li X, Zhang Y, Zhang Y, et al (2008). RUNX3 inhibits growth of HCC cells and HCC xenografts in mice in combination with adriamycin. *Cancer Biol Ther*, **7**, 669-76.

Livak KJ, Schmittgen TD (2001). Analysis of relative gene expression datausing real-time quantitative PCR and the 2-Ct method. *Methods*, **25**, 402-8.

Miyazono K, Suzuki H, Imamura T (2003). Regulation of TGF-beta signaling and its roles in progression of tumor. *Cancer Sci*, **94**, 230-4.

Mori T, Nomoto S, Koshikawa K, et al (2005). Decreased expression and frequent allelic inactivation of the RUNX3 gene at 1p36 in human hepatocellular carcinoma. *Liver Int*, **25**, 380-8.

Nakanishi Y, Shiraha H, Nishina S, et al (2011). Loss of runt-related transcription factor 3 expression leads hepatocellular carcinoma cells to escape apoptosis. *BMC Cancer*, **11**, 3.

Sakakura C, Hasegawa K, Miyagawa K, et al (2005). Possible involvement of RUNX3 silencing in the peritoneal metastases of gastric cancers. *Clin Cancer Res*, **11**, 6479-88.

Shiraha H, Nishina S, Yamamoto K (2011). Loss of runt-related transcription factor 3 causes development and progression of hepatocellular carcinoma. *J Cell Biochem*, **112**, 745-9.

Tsunematsu T, Kudo Y, Iizuka S, et al (2009). RUNX3 has an oncogenic role in head and neck cancer. *PLoS One*, **4**, e5892.

Wei D, Gong W, Oh SC, et al (2005). Loss of RUNX3 expression significantly affects the clinical outcome of gastric cancer patients and its restoration causes drastic suppression of tumor growth and metastasis. *Cancer Res*,

65, 4809-16.
Zhang S, Li ZF, Pan D, et al (2009). Changes of splenic macrophage during the process of liver cancer induced by diethylnitrosamine in rats. *Chin Med J*, **122**, 3043-7.